Transient Finite Element Analysis of a SPICE-coupled Transformer with COMSOL Multiphysics

T. Bödrich [*1], H. Neubert [1], and R. Disselnkötter [2]
[1] Institute of Electromechanical and Electronic Design, Technische Universität Dresden, Germany,
[2] ABB AG, Forschungszentrum Deutschland, Germany
* Corresponding author: TU Dresden, IFTE, 01026 Dresden, Germany, Thomas.Boedrich@tu-dresden.de

Abstract: The operation of transformers is characterised by strong dynamic interactions between the magnetic system and the electric circuits that are connected to the primary and secondary windings. Transient finite element modelling (FEM) of the transformer with coupling to SPICE circuit models containing the electrical sources and loads is a powerful means for analysis and design. This paper describes the approach followed in COMSOL with 3D magnetic FEM and transient simulation of a current transformer with a non-linear core characteristic that has both windings coupled to external circuitry via a SPICE netlist. This is a configuration which is quite challenging with respect to numerical stability. Further focus is on how to model the multi-turn winding.

Keywords: transformer, transient analysis, 3D finite element model, SPICE, non-linear ferromagnetic material

1. Introduction

Current transformers (CTs) are used to measure currents in power distribution and control systems. Their purpose is to precisely transform the high power line current (which may range from a few A up to several kA) into a much smaller current or voltage that can be easily measured. Typically, the primary winding of such a transformer will consist of just a single turn (cable or bus bar) with a high cross-section, whereas the secondary is composed of many loops of thin wire. In order to achieve a low current error with a transformer factor close to the winding ratio, the secondary winding needs to be operated on a small load resistance close to short-circuit conditions. This will also lead to a low overall transformer impedance and prevent the occurrence of high voltages on the secondary side [1]. Although the use of a small load resistance and a highly permeable core material will reduce the core flux density, and further the magnetic losses and current error in the major part of the operating regime, the non-linearity of the core material and beginning saturation effects may come into play in certain regions of cores with more complex shapes at least close to the limits of the operating ranges. More complex core geometries are encountered for example with stacked core transformers or with non-conventional CTs that use additional flux sensors, air gaps and electronic circuitry to extend their frequency operating range down to DC.

In such cases, finite element analysis (FEA) can help in the design process to investigate and modify the flux density distribution in the transformer core especially with high primary currents, where core saturation must be avoided.

2. Finite Element Model of the Transformer

Figure 1 shows the shape of a 3D CT-test structure which was modelled and analysed in COMSOL. As a peculiarity of this device, the ferromagnetic core has a square frame-structure and contains a full air gap in the top core branch. It can be expected, that this will induce stray fields and thereby a reduced coupling between the primary and secondary windings of the transformer. Additionally, there is a partial gap in the right section, which does not fully separate the core. Since the dimensions of the gaps are much smaller than those of the frame, many mesh elements will be required for an accurate model. Due to the asymmetric configuration of the two gaps, symmetry conditions can not be exploited for a reduction of the FE-model down to a geometry sub-group in order to keep it small. Hence, a complete 3D transformer model is required.

While the primary winding consists of only one turn (a straight bus bar running through the centre of the frame), the secondary is composed of two linear coils with rectangular cross-section and 500 turns each, which are connected in se-

ries. Hence, the total number of secondary wire loops is $N = 1000$. Instead of modelling each of them separately, the two partial windings are modelled with a total of eight bulk prismatic bodies according to Figure 1.

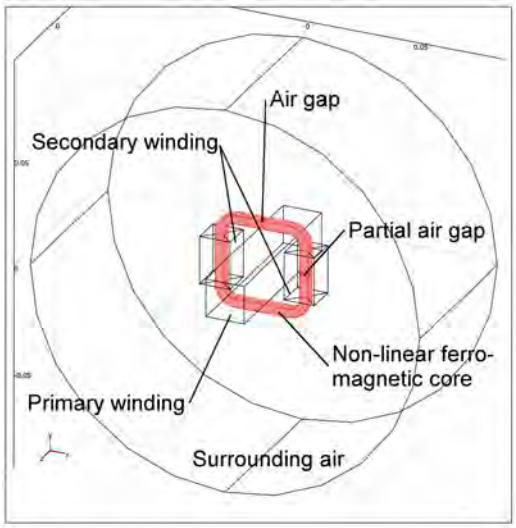

Figure 1. Geometry of the 3D transformer test model

The primary conductor is modelled as a single copper block. A homogenous current density distribution

$$J_1(t) = \frac{i_1(t)}{A_{\text{prim}}} \tag{1}$$

with $i_1(t)$ denoting the primary current according to Section 3 and A_{prim} being the cross-sectional area of the primary conductor is fed into the latter as an external current density $\boldsymbol{J}^{\text{e}}$ (Figure 2). Likewise, a secondary current density

$$J_2(t) = \frac{N\, i_2(t)}{A_{\text{sec}}} \tag{2}$$

with $i_2(t)$ denoting the secondary current calculated during transient simulation, N being the total number of secondary turns, and A_{sec} being the total cross-sectional area of the secondary winding is fed into each of the eight subdomains of the secondary winding as a homogenous external current density $\boldsymbol{J}^{\text{e}}$ with the respective local orientation and polarity (Figure 2). Due to the constant height of the prismatic elements, current continuity will be preserved at the 45° interfaces even though there is a change in direction.

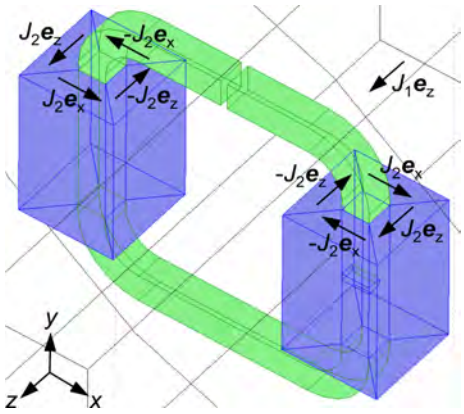

Figure 2. Homogeneous current densities J_1 in the primary winding and J_2 in the 2 x 4 prismatic bodies that form the secondary winding

For reasons of numerical stability and low computational effort, the element type Vector–Linear is assigned to all subdomains of the model. Free meshing is applied based on the predefined mesh size 'Coarser' (Figure 3). Only the four curved surfaces at the inner side of the core frame are manually restricted to a maximum element size in order to avoid inverted elements. This meshing results in only 6,604 elements and 7,985 degrees of freedom with the chosen application mode 'Induction Currents' (emqa; see Section 4). The rather low resolution is selected here for a fast and stable convergence of the solution without the need of a tedious model optimization process. For more detailed results the mesh resolution needs to be improved. It can then be more difficult to achieve a stable simulation performance in wide frequency and amplitude operating ranges for a model with this combination of properties and couplings. However, we also succeeded in simulating models of the same type with mesh size "Normal" and more than 50,000 degrees of freedom on a standard laptop in COMSOL Multiphysics 3.5a.

Meshing of selected subdomains with other types of elements and techniques (hexahedral; mapped, extruded and swept meshes) has been tested as an alternative but did not lead to improvements so far.

In order to investigate the effects of local core saturation at high current amplitudes, the non-linear $B(H)$-characteristic of the core material needs to be taken into account. In this example a high permeability Iron Silicon alloy is selected (Figure 4).

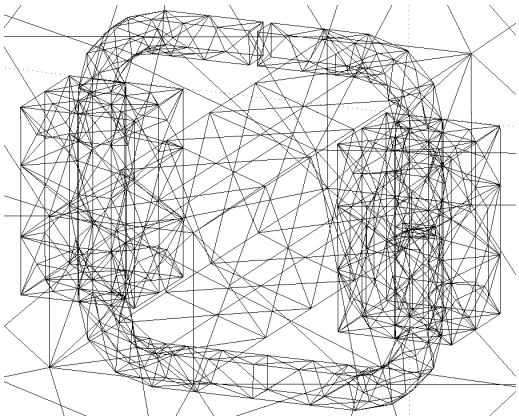

Figure 3. Meshing of the boundary elements of the transformer (with predefined mesh size "Coarser")

In order to avoid circular variable definitions in the constitutive relations [2], the core characteristic must be described in the less common form $\boldsymbol{H}=f(|\boldsymbol{B}|)\boldsymbol{e}_{\boldsymbol{B}}$. Beyond the magnetic saturation of the core material the characteristic needs to be extrapolated with the differential relative permeability of air ($\mu_{r\,diff}=1$) up to very high amplitudes of the magnetic field [2] (Figure 5) to assure a controlled asymptotic behavior during the convergence process of the solution.

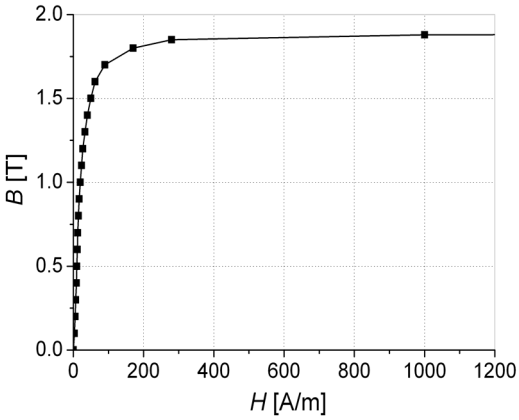

Figure 4. Magnetisation curve $B(H)$ of the simulated core material silicon iron

At present, eddy currents in the core and the primary and secondary windings are still suppressed for reasons of simplicity (see Section 4) by setting the conductivity to $\sigma=10$ S/m in all of the subdomains. This will probably be changed in future versions of the model.

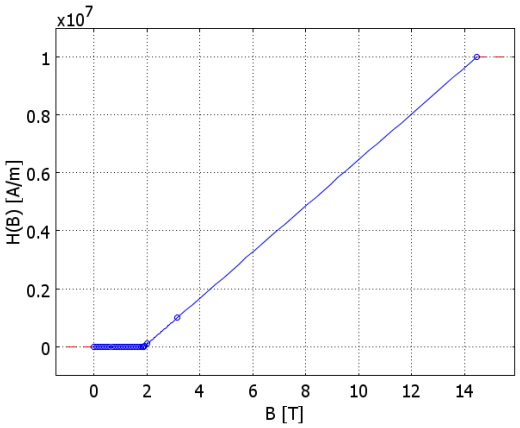

Figure 5. Extrapolated curve $H(B)$ for the core material silicon iron as used in the simulations

3. Coupling with SPICE Components

The circuit shown in Figure 6 is coupled to the FE model of the CT via a SPICE netlist. It has been used in the transient simulations of the test model. For modelling realistic applications it could be replaced by more complex circuitry on both the primary and secondary sides of the CT.

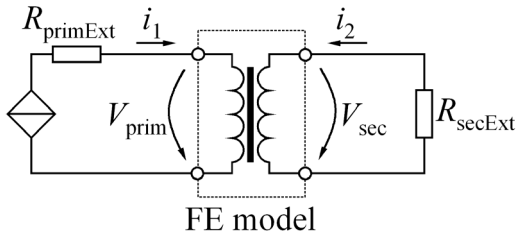

Figure 6. SPICE circuit coupled to the FE model of the transformer

The above circuit is implemented in COMSOL Multiphysics 3.5a as follows (Physics ⇒ SPICE Circuit Editor…):

```
I1source 0 1 sin(0 1000 50)
RprimExt 1 2 1
X1 2 0 primFEM
X2 3 0 secFEM
RsecExt 3 0 1
.SUBCKT primFEM Vprim i1 COMSOL: *
.ENDS
.SUBCKT secFEM Vsec i2 COMSOL: *
.ENDS
.END
```

A sinusoidal 50 Hz current

$$i_1(t) = 1000\,\mathrm{A}\,\sin(2\pi\,50\,\mathrm{s}^{-1}\,t) \qquad (3)$$

with a peak value of 1000 A is fed into the primary winding. Although the external resistor $R_{\mathrm{primExt}} = 1\ \Omega$ would not be needed in conjunction with a current source, it is here included in the primary circuit to improve the numerical stability, as the primary impedance of the "short-circuited" CT is low. On the secondary side, an external shunt resistor $R_{\mathrm{secExt}} = 1\ \Omega$ is connected directly to the winding terminals. It will generate the CT output voltage. The ohmic voltage drop in the secondary winding itself is accounted for by the definition of the coil resistance $R_{\mathrm{coil}} = 4\ \Omega$ in the FE model under Options ⇒ Constants. Then, the voltage V_{sec} across the secondary terminals is defined under Options ⇒ Expressions ⇒ Global Expressions:

$$V_{\mathrm{sec}} = R_{\mathrm{coil}} \cdot i_2 - V_{\mathrm{i}} \qquad (4)$$

$$V_{\mathrm{i}} = \int_l \boldsymbol{E}\,\mathrm{d}\boldsymbol{l} = \frac{N}{A_{\mathrm{sec}}} \cdot \sum_{k=1}^{8} K_k \qquad (5)$$

Here, V_i is the voltage induced in the complete secondary winding. It corresponds to the line integral of the electric field strength $\boldsymbol{E}$ along the total length l of the wire. In the case of a bulk winding model as implemented in the presented example, it can be derived from the sum $K_1 + K_2 + \ldots + K_8$ of the volume integrals

$$K_k = \int_{V_k} \boldsymbol{E}_k\,\mathrm{d}V \qquad (k = 1, 2, \ldots, 8) \qquad (6)$$

where $\boldsymbol{E}_k$ is the amplitude of the electric field component in the direction of the current in the k^{th} prismatic subdomain of the secondary winding. This is defined in Options ⇒ Integration Coupling Variables ⇒ Subdomain Variables: Ex_emqa and Ez_emqa, where the field components are chosen according to the orientation of the imposed external current density J_2 (see Figure 2).

4. Transient Simulation

Transient simulations of 3D quasi-static magnetic field problems with COMSOL Multiphysics 3.5a require the selection of the application mode emqa (Induction Currents) [3]. The simulation of the described model was performed on a PC with an Intel Core2 Quad CPU 2.40 GHz and 8 GB RAM. The settings

Solver:	Time dependent
Time range:	0.06 s (three 50Hz-periods)
Linear system solver:	Direct (PARDISO)
Rel. tolerance:	10^{-6}
Abs. tolerance:	10^{-8}

and the above-mentioned 7,985 degrees of freedom resulted in a solution time of 442 s.

The transient response obtained in the simulations is shown in Figure 7. The comparison of the induced secondary current i_2 with the primary current shows, that due to the deliberately chosen design of the test CT it has only low accuracy at the given amplitude and frequency of the primary current. A number of shortfalls are evident: a significant deviation from the ideal transformer ratio of 1:1000, initial transient effects and a positive phase shift of the secondary current, which are consequences of the imperfect coupling between the windings resulting from the rather large full air gap.

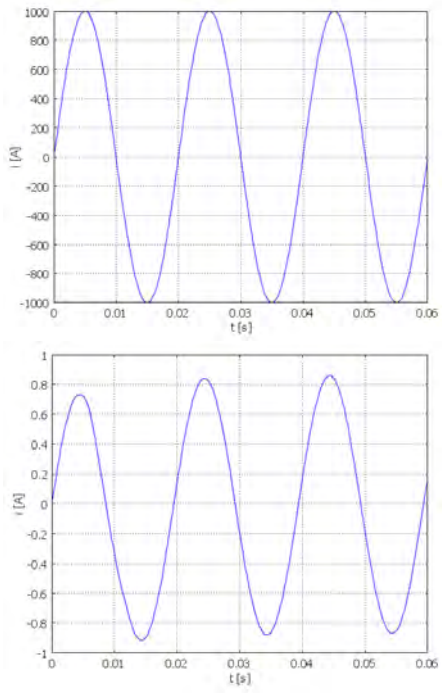

Figure 7. Simulation results: primary current i_1 imposed by the current source (top) and induced secondary current i_2 (bottom)

In addition to analyzing the output signal of the CT and its overall performance, the simulations also offer the possibility for a better understanding of the phenomena by having a closer look at the flux density distribution within the magnetic core at different points in time. Figure 8 reveals the local impact of demagnetizing fields resulting from the full air gap and the secondary windings at the moment when the primary current is at its maximum: It can be seen, that in the affected core sections the induction is much lower than in the bottom branch.

Another snap-shot taken during a zero-crossing of the primary current shows that due to the phase shift between the currents there will be still a high induction level in the remaining part of the partial gap at this time (Figure 9).

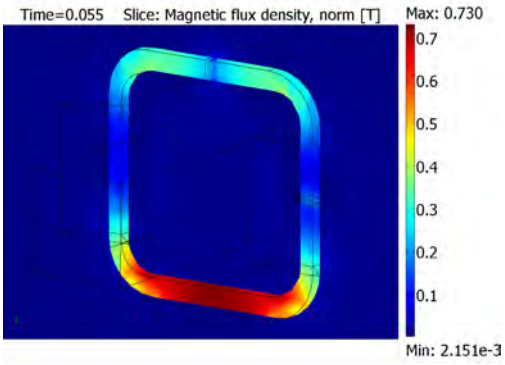

Figure 8. Snap-shot of the magnetic flux density distribution (absolute value) in the centre plane of the CT core frame at maximum primary current amplitude (full air gap at the top, partial gap in the right core section)

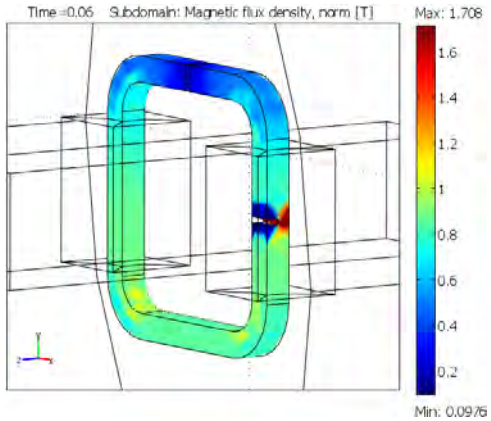

Figure 9. Snap-shot of the flux density distribution (absolute value) on the surface of the CT core during zero-crossing of the primary current

5. Summary and Outlook

It has been shown that FEA can help in the analysis and understanding of the transient behaviour and the generated flux density distributions in complex 3D transformer geometries during the design process. The presented model of a transformer test structure allows transient simulations with coupling to external circuitry by means of a SPICE netlist. The non-linear magnetisation characteristic of the core material is taken into account with a relationship $\boldsymbol{H}=f(|\boldsymbol{B}|)\boldsymbol{e_B}$ that is defined via a table. The secondary winding, which typically consists of many turns, is modeled as a bulk region into which a homogeneous external current density distribution is injected.

Focus of future work will be on improvement of the numerical stability of the models in order to extend their stable current amplitude and frequency ranges. Further, a reduction of the mesh size is desired in cases where the influence of small structures, like small air gaps or core laminations needs to be analysed. This will lead to an increased number of degrees of freedom, and a change-over to iterative solvers may be required for best memory efficiency.

So far, eddy currents have been excluded from the investigations although they are playing an important role in many of the applications. Therefore, it will be another goal for the future to integrate the effects of eddy currents on bulk or laminated cores and windings into the transformer models.

References

1. G. Müller: *Elektrische Maschinen – Grundlagen, Aufbau und Wirkungsweise*, 7th ed., Verlag Technik, Berlin (1989)
2. COMSOL AB: *Support Knowledge Base 852– How can I model nonlinear magnetic materials?,* http://www.comsol.com/support/knowledgebase/852/ (Sep. 10, 2010)
3. COMSOL AB: *AC/DC Module – User's Guide*, p. 151 (COMSOL 3.5a, 2008)